Supporting Information

Differential Hysteresis Scanning of Non-Templated Monomodal Amorphous Aerogels

Poroshat Taheri,† John C. Lang,† Jeffrey Kenvin,‡ Peter Kroll†

† Department of Chemistry & Biochemistry, The University of Texas at Arlington, Arlington, TX 76019 USA

‡ Micromeritics Instrument Corporation, 4356 Communications Drive, Norcross, Georgia, 30093, USA

1. Additional Observations

1.1 Hysteresis Loop Non-Closure

One of the features common to these unannealed SiCO materials (pa's) and their preparation, is their open-ended hysteresis loops, characterized in the Porosity portion of the Results section. There it was observed that the adsorption and desorption arms of the isotherm did not merge, even at a P/P_0 of 0.22.[1] A frequent explanation of this effect is entrapment of adsorbate in micropores or ultra-micropores.[2, 3] Here, for the four evaluations, with both nitrogen and argon as adsorbates, the t-plot assessment of microporosity showed negative intercepts and negligible microporosity. Another explanation for non-closure has been surface effects that slow the rate of adsorbate evaporation and equilibration. We explored this possibility by redetermining the nitrogen isotherm for **pa-a**, whose absolute difference in specific volumes was greater, using parameters that slowed the rate of data acquisition. The isotherm is shown in SI-Figure 1.
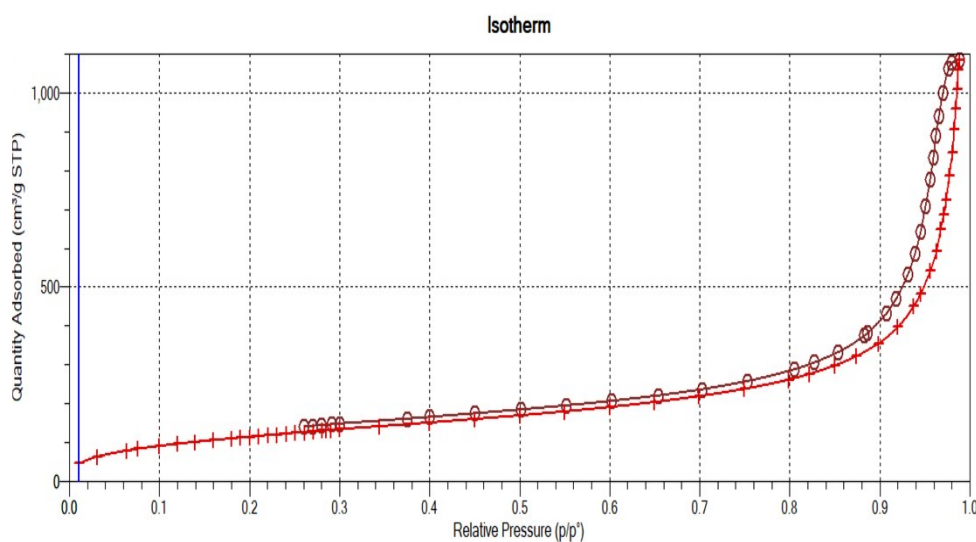
SI-Figure 1. Nitrogen **i**sotherm for **pa-a**, to be compared with the more rapidly acquired single isotherm in Figure 3A (solid line).

Both the equilibration intervals and equilibration delay times were increased significantly for this evaluation and the screen shot of these settings as specified in the ASAP 2020 system software as are shown in SI-Figure 2.

SI-Figure 2. Screen shot of the Equilibration window as it was specified under the Analysis Conditions in the ASAP 2020 software for the reanalysis of sample **pa-a**.
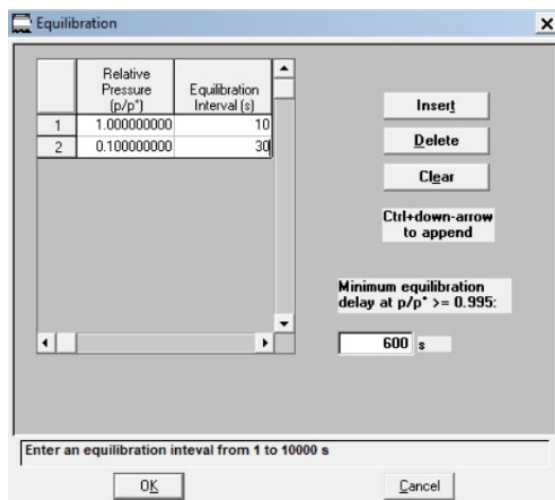
The isotherms shown in Fig. 3A and SI-Figure 1 are essentially indistinguishable. The non-closure was evaluated by selecting three points in the plateau regions for each isotherm, averaging the differences in specific volumes between the two arms of the isotherms, and evaluating their differences with a t-test that indicated there was only a 3% chance that the two isotherms are different.

We concluded that, at least by this measure, the kinetics of desorption were not the likely source of non-closure.

There are several other sources of non-closure, which as we indicated are common in this family of materials. From the BET C values listed in Table 1 it is readily apparent for the annealed ceramic samples, where there is complete closure, that significant increases in C have accompanied the annealing. Such transformations of surface energy could well influence the wetting behavior.[3] Abundant literature suggests this might well influence the openness between the two arms of the isotherm.[4] Additionally, it is well-known that annealing, while not melting the ceramic, can lead to "ripening" of the particles, an effect that will remove inherent roughness of the particulate aggregates. Both local energetics and wetting can be influenced, again with potential impact on the hysteresis closure.[5] Assessing surface roughness can be routinely investigated using scattering techniques,[6] and the characteristic evolution of structure accompanying sintering of porous xerogels serves as an example.[7, 8]

These effects are topics of continuing research.

1.2 Relative Volumes

Simply, to distinguish the difference between the absolute shape-attributed specific volumes from the measurement from the relative values normalized with respect to the total pore **pa-a** provided in Table 2, we have included here in SI-Table 1 the Specific Volumes (in cm3 g-1 STP) reported by the DHS software, and in the last column their sum, the basis for the normalization.

SI-Table 1. Specific pore volumes attributed to the characteristic pore geometries for the four Si-CO's.

Sample	Specific Volume Pyr (cm^3 g^{-1})	Specific Volume Con (cm^3 g^{-1})	Specific Volume Occ (cm^3 g^{-1})	Sum
pa-c	0.048	0.472	0.022	0.542
ca-c	0.024	0.122	0.013	0.159
pa-a	0.274	0.682	0.031	0.987
ca-a	0.144	0.517	0.063	0.724

1.3 Pore Morphologies and Organization

In the discussion at the end of §3.3, following Figure 5, the appearance of the contour plots for sample **pa-c** led to the supposition that this bimodal distribution of pore geometries might be occurring through windows of the same size, and this could be interpreted to indicate both pore sizes share the same window. For clarification of the implications of this conjecture we have included a few figures to suggest constraints this might impose on the organization of the pores in the constituent particles, such as those reported in Figure 3. These organizational constraints are imposed by the observation that after annealing the larger pores are still accessible to adsorbate. The next figure, SI-Figure 3, provides colored representations of the two pore size distributions, simplified as blue for the large pores, and red for the smaller pores. The gray sheet represents the surface of the particles where the windows are located.
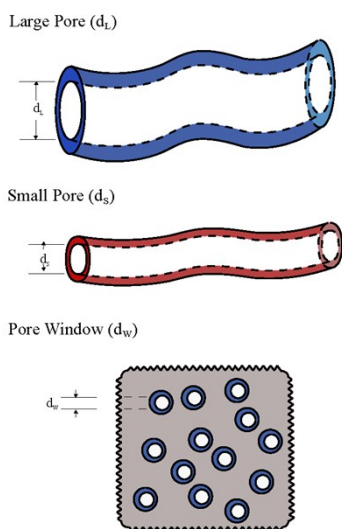
SI-Figure 3. Schematic representation of the pores comprising the bimodal distributions, with the larger blue pores having a diameter d_L, which in Figure 5 is centered at about 40 nm, and the smaller red pores having a diameter d_S, which in Figure 5 is centered at about 20 nm. In the Figure to the left the pore window with diameter designated d_W, which in Figure 5 is about 10 nm, is indicated to open onto only one size of pore.

The color coding in the second figure, SI-Figure 4, provides some suggestions of possible arrangements of the pores if the conjecture of a shared window is appropriate. In SI-Figures 4a and b there are three distinct regions: the outer surface **s**, the location of the window, a corona for the first layer, and a core. In both representations only one pore size occurs in an entire region. In 4a the corona is the large pore and the core the small pore; in 4b the sequence is reversed. In SI-Figure 4c, both large and small pores are occurring in both the corona and the core, hence the blended color. But even here there are constraints from the results following annealing and collapse of the small pores. To discuss these, one such acceptable organization is proposed in SI-Figure 4d.
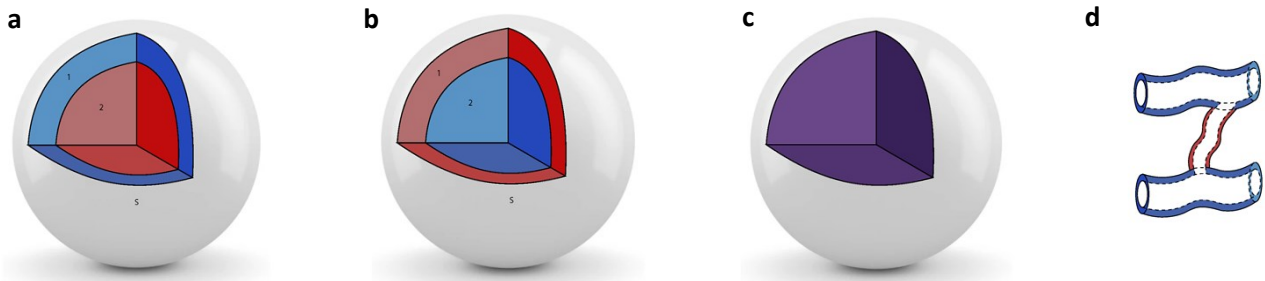
SI-Figure 4. Figures **a-c** are representations of the distinct particles shown in the SEMS of Figure 2. The "spheres" have an octant cut from the solid so that the composition of the interior can be explored. Possible arrangements are discussed in the following text. Figures **a** and **b** define three zones, s is the surface, 1 the outer region just inside the surface, and 2 the core inner region. Figure **d**, based on the two pore types shown in SI-Figure 3, is simply suggestive of one arrangement, one with intersecting pores that would be consistent with the pattern of Figure **c**, with a uniform consistent pattern of pores throughout the interior of the particle. Here, as in SI-Figure 3, the windows are expected to be located on the surface of the particle.

Here we define these different types of configurations symbolically to facilitate discussion. Figures **a** and **b** in SI-Figure 4 are complementary, each have two **S**erial zones of segregated pores. In Figure a, the larger pores are restricted to the outer zone and the smaller, to the inner zone. This is configuration **S-1** with likelihood assigned as F_1. In Figure b, the arrangement is reversed with the smaller pores restricted to the outer zone. This is configuration **S-2** with likelihood F_2. Given the observation that on annealing the smaller pores are envisioned to collapse yet leave the large pores still accessible, arrangement **b** seems highly unlikely, whereas arrangement **a** seems quite acceptable, i.e., $F_1 >> F_2$.

This brings us to arrangement c, the "homogeneous", single-zone depiction encompassing both large and small pores. Because of the number of possibilities that are consistent with such a uniformity we have summarized these in SI-Table 2.

SI-Table 2. Potential arrangements of large and small pores in the "homogeneous" region depicted in SI-Figure 4c. For the Parallel Configuration, Zones 1 and 2 correspond to their location in SI-Figures 4a and b that is as corona and core respectively, or for Figure **c** simply the sequential organization. For the Intersecting Configuration, Longitudinal and Transverse refer to paths nominally perpendicular to the surface or between two perpendicular pores , respectively. The transverse direction is suggested by the orientation of the smaller pore illustrated in SI-Figure 4d. The likelihood of these arrangements is suggested.

Configuration	Window	Zone 1	Zone 2	Likelihood
Parallel (P-1)	W_S W_L	d_S d_L	d_S d_L	F_3
Intersecting		Longitudinal	Transverse	
I-1	W_S	d_S	d_L	F_4

I-2	W_L	d_L	d_S	F_5
I-3	W_L	d_L	d_L & d_S	F_6

From the arguments discussed above, F_2 and F_4 are highly unlikely, whereas conversely, F_1, F_5, and F_6 would appear to be more likely. While the parallel configuration is possible, such segregation during synthesis seems improbable. The ranking appears to be F_2 & $F_4 < F_3 < F_1 < F_5 < F_6$. The latter two are ranked simply based on the expectation that some of the intersecting crosslinks need not be exclusively the small pores.

By enumerating the network connectivity[9] taken to only a single tier of hierarchy for a simple bimodal distribution of pore sizes it is also clear why there might be little expected change in pore volume for the distribution of the larger pores. First, as suggested in Figure SI-4d, let there be just two types of pores, those connected to the surface (P_s) and those interconnecting two pores (P_c). For those connected to the surface, there are two options based on size, $P_s(L)$ and $P_s(S)$. For the connections, there are three options, $P_s(L)$, $P_s(S)$ and $P_s(O)$, where the latter indicates no interconnection. From assessing the assortment of P_s pairs and the variety of P_c interconnections, there are only nine sets of these primary pore types. Neglecting the differences in pore areas and volumes of these different types of pores, there are twenty-four appearances of pore locations. However, only one of the twelve affecting the large pores would reduce adsorption resulting from complete occlusion and collapse of the small pores.

SI References:

1. D. Everett, in *The Solid-Gas Interface*, ed. E. Flood, Marcel Dekker, Inc., New York, 1967, vol. 2, ch. 36, pp. 1055-1113.
2. K. Morishige and M. Ishino, *Langmuir*, 2007, **23**, 11021-11026.
3. L. D. Gelb, K. Gubbins, R. Radhakrishnan and M. Sliwinska-Bartkowiak, *Rep. Prog. Phys.*, 1999, **62**, 1573.
4. S. Gregg and K. Sing, *Adsorption, surface area and porosity. Academic Press, London*, 1982.
5. H. Tanaka, T. Hiratsuka, N. Nishiyama, K. Mori and M. T. Miyahara, *Adsorption*, 2013, **19**, 631-641.
6. A. Chatterjee, R. K. Kalia, A. Nakano, A. Omeltchenko, K. Tsuruta, P. Vashishta, C.-K. Loong, M. Winterer and S. Klein, *Appl. Phys. Lett.*, 2000, **77**, 1132-1134.
7. V. A. Hackley, M. A. Anderson and S. Spooner, *J. Mater. Res.*, 1992, **7**, 2555-2571.
8. C. J. Brinker and G. W. Scherer, *J. Non-Cryst. Solids*, 1985, **70**, 301-322.
9. N. Seaton, *Chem. Eng. Sci.*, 1991, **46**, 1895-1909.